Earth and Planetary Science Letters 351–352 (2012) 237–246

Contents lists available at SciVerse ScienceDirect

Earth and Planetary Science Letters

journal homepage: www.elsevier.com/locate/epsl

Multi-stage exhumation of young UHP–HP rocks: Timescales of melt crystallization in the D'Entrecasteaux Islands, southeastern Papua New Guinea

S.M. Gordon [a,*], T.A. Little [b], B.R. Hacker [c], S.A. Bowring [d], M. Korchinski [b], S.L. Baldwin [e], A.R.C. Kylander-Clark [c]

[a] Department of Geological Sciences, University of Nevada, Reno, NV, USA
[b] School of Earth Sciences, Victoria University of Wellington, New Zealand
[c] Earth Research Institute, University of California, Santa Barbara, CA, USA
[d] Department of Earth, Atmospheric, and Planetary Sciences, Massachusetts Institute of Technology, Cambridge, MA, USA
[e] Department of Earth Sciences, Syracuse University, Syracuse, NY, USA

ARTICLE INFO

Article history:
Received 10 February 2012
Received in revised form
11 July 2012
Accepted 12 July 2012
Editor: T. M. Harrison
Available online 31 August 2012

Keywords:
eclogite
partial melting
exhumation
CA-TIMS
Papua New Guinea

ABSTRACT

On the D'Entrecasteaux Islands, southeastern Papua New Guinea (PNG), a series of domes expose the youngest known ultrahigh-pressure (UHP) to high-pressure eclogites and associated gneisses. Abundant evidence of partial melting is preserved throughout the D'Entrecasteaux domes in the form of variably deformed leucosomes, dikes, and plutonic bodies. In order to understand (1) the timing of melt emplacement relative to the UHP metamorphism and (2) the complete exhumation and deformational history of the eclogites and surrounding gneisses, a series of leucosomes, dikes, and eclogites from the Mailolo dome in western Fergusson Island were analyzed by U–Pb ID-TIMS zircon geochronology. Zircons extracted from the eclogite at the UHP locality yield $^{206}Pb/^{238}U$ TIMS dates from 5.60 ± 0.22 to 4.61 ± 0.18 Ma. Zircons from three foliation-parallel leucosomes are interpreted to record melt crystallization from 3.49 ± 0.01 Ma to 2.98 ± 0.02 Ma. In comparison, weakly deformed granitic–granodioritic dikes that cut the leucosomes yield zircon $^{206}Pb/^{238}U$ dates of 2.48 ± 0.01 Ma–2.420 ± 0.002 Ma. Based on these new and previously published results, the eclogites may have undergone UHP metamorphism for several million years, from 7.1 ± 0.7 Ma to 4.61 ± 0.18 Ma; based on TIMS dates alone, a more restricted interval of 5.6–4.6 Ma is proposed. Following UHP metamorphism, the eclogite and gneisses were exhumed to lower crustal depths, intruded by foliation-parallel leucosomes by ca. 3.5–3.0 Ma and by ca. 2.45 Ma late discordant dikes. Multiple generations of leucosomes and dikes allow a timeline for the exhumation of the PNG UHP terrane to be constructed: mantle (~100 km depths) to the base of the crust in ~1 my, storage in the lower crust for ~1 my, and final emplacement into the shallow crust ~1 my later.

1. Introduction

Evidence from a variety of different isotope systems (e.g., carbon: Sobolev and Sobolev, 1980; Sobolev, 1984; sulfur: Chaussidon et al., 1987; lead: Armstrong, 1991; Eldridge et al., 1991) suggests that crustal material is recycled into the mantle despite its low density (e.g., Schreyer, 1995). Some of the crustal rocks that are subducted to mantle depths return to the surface and are exposed in ultrahigh-pressure (UHP) terranes. Rare eclogites and gneisses in UHP terranes contain coesite, indicating pressures > ~ 27 kbar or ~100 km depths (e.g., Chopin, 1984; Smith, 1984). Even rarer diamond inclusions suggest that crust locally reached even greater pressures/depths (> 40 kbar/130 km) before being returned to Earth's surface (e.g., Sobolev and Shatsky, 1990; Dobrzhinetskaya et al., 1995; Nasdala and Massone, 2000). Most geodynamic models argue for buoyancy as the main force exhuming these rocks at least to the base of the crust (e.g., Ernst et al., 1997; Ernst and Liou, 2000; Gerya and Stöckhert, 2006; Warren et al., 2008).

Some UHP terranes achieved higher temperatures than predicted by models for subduction of oceanic lithosphere (Syracuse et al., 2010)—temperatures at which mica undergoes dehydration melting (Hacker, 2006). Crustal rocks in the Kokchetav Massif and the Bohemian Massif are interpreted to have reached such temperatures, > 1000 °C (Shatsky et al., 1995; Zhang et al., 1997; Massone, 1999) and to have undergone anatexis, resulting

* Corresponding author. Tel.: +1 775 784 6476.
E-mail address: staciag@unr.edu (S.M. Gordon).

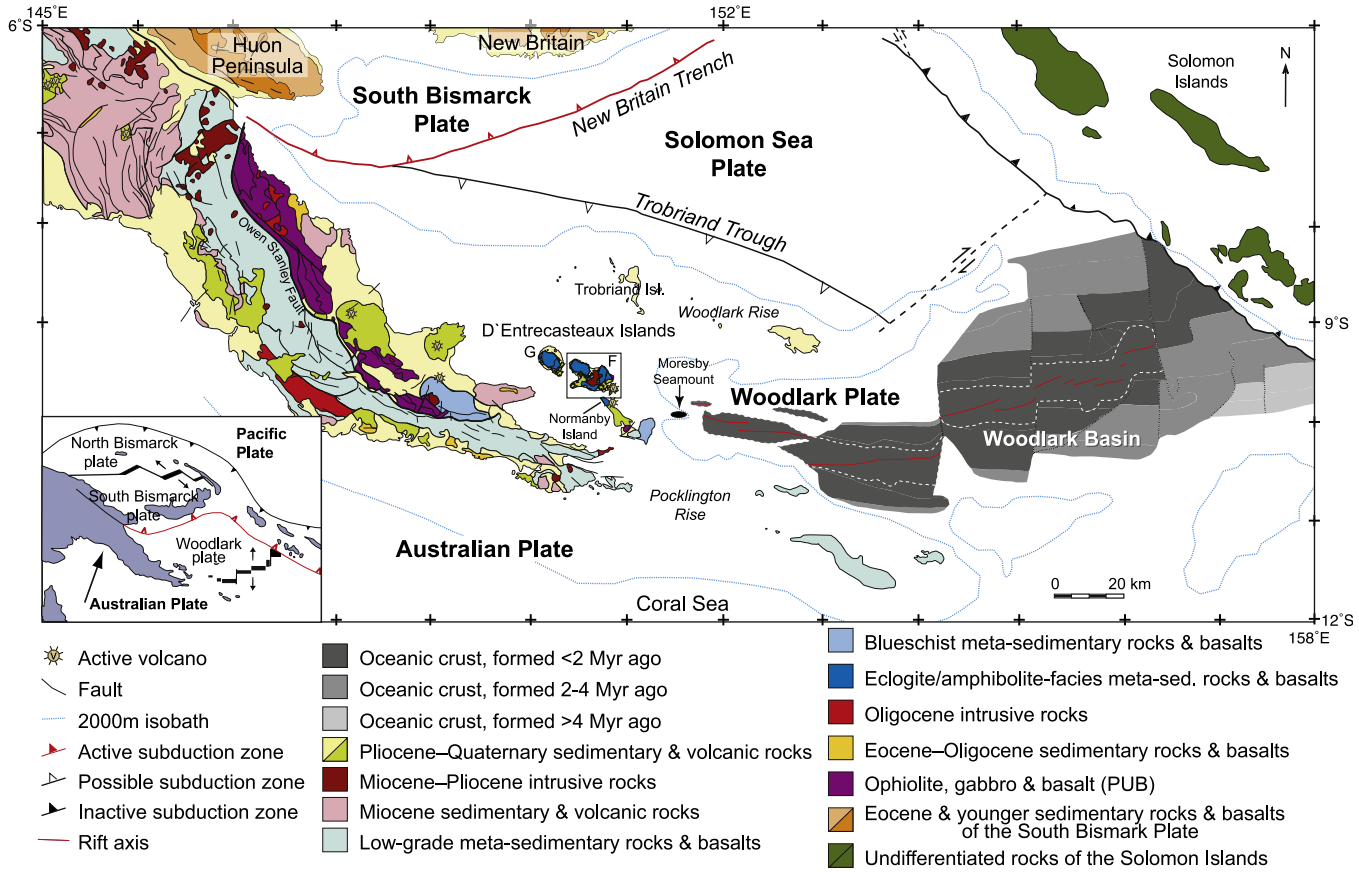

Fig. 1. Tectonic and geologic map of eastern Papua New Guinea showing the major rock units, structures and the location of the D'Entrecasteaux Islands (after Baldwin et al., 2004). Also shown is the location of the Woodlark basin, where sea-floor spreading transitions to the west into continental rifting. The white-dashed line shows the location of the Bruhnes chron. The box shows the location of the geologic map presented in Fig. 2. Inset: contemporary plate tectonic map of eastern Papua New Guinea. G: Goodenough Island; F: Fergusson Island; PUB: Papuan ultramafic belt.

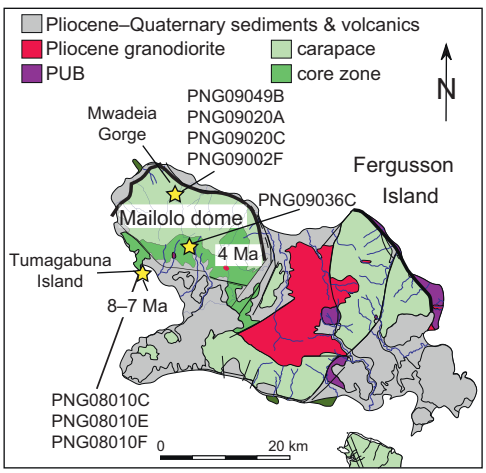

Fig. 2. Geologic map of Fergusson Island, part of the D'Entrecasteaux Islands (after Hill, 1994; Little et al., 2007). The map shows the main structural zones of the domes: the carapace and core zone. The map also shows the location of the collected samples and the interpreted ages of UHP–HP metamorphism dated by U–Pb ion microprobe and Lu–Hf (ages from Baldwin et al., 2004; Monteleone et al., 2007; Zirakparvar et al., 2011).

in a buoyant melt/crystal mush that ascended from >200 km depth (Massone, 2003). Most UHP terranes do not record such high temperatures, but do contain large tracts of migmatitic gneiss hosting eclogite (e.g., Labrousse et al., 2011). Little is known about the timescales and effects of partial melting (e.g., <30% melt produced) of continental crust during subduction to and exhumation from mantle depths.

In eastern Papua New Guinea (PNG), Pliocene UHP–HP eclogites are contained in migmatitic host gneisses (Figs. 1 and 2). The PNG UHP terrane is unique in that it is exposed within an active, rapidly extending (>20 mm/yr) continental rift, the Woodlark Rift (Fig. 1; Ruppel, 1995; Abers, 2001; Wallace et al., 2004). In addition, this terrane may have the largest volume of crystallized partial melt of all UHP terranes, with (a) abundant leucosomes (~10–20 vol.% of most outcrops and up to 40 vol.% in the core of at least one dome), (b) dm- to m-thick dikes (5–70 vol.% of the outcrop), and (c) large (tens of km in diameter) granodioritic to leucogranitic plutons (Figs. 3; Table 1).

The migmatites and eclogites exposed in PNG represent an excellent locality to determine when the leucosomes and dikes crystallized and how melting was related to deformation and rapid exhumation. Unlike most older examples, the PNG UHP terrane has not been overprinted by a younger orogenic event. Here we report new U–Pb zircon chemical-abrasion isotope-dilution thermal ionization mass spectrometry (CA-TIMS) and laser-ablation inductively coupled plasma mass spectrometry (LA-ICPMS) zircon results that reveal the timescales of melt crystallization and deformation relative to the timing of UHP–HP metamorphism. The new geochronology identifies multiple generations of melt that crystallized during a few million years of Pliocene exhumation.

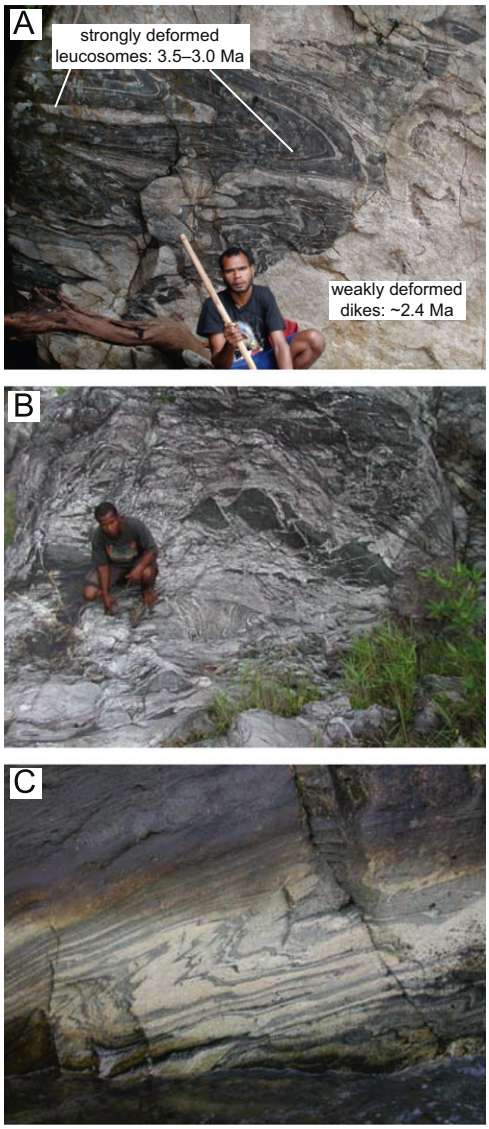

Fig. 3. Field photos revealing the abundant leucosomes and dikes found throughout the D'Entrecasteaux Islands: (A) outcrop structures of the two main types of leucosomes and dikes from the Mailolo dome carapace: (1) strongly deformed, layer-parallel leucosomes yield ~3.5–3.0 Ma crystallization dates; and (2) weakly deformed, discordant dikes yield ~2.4 Ma crystallization dates. The area marked as the weakly deformed, discordant dike is where PNG0920C was collected; (B) Goodenough Island outcrop, PNG06034, that contains 69 vol.% crystallized dike (Table 1); and (C) Goodenough Island outcrop, PNG06039, that contains 54 vol.% crystallized dike (Table 1).

2. Geologic setting

2.1. Regional context

The 10–11 cm/yr convergence between the Australian and Pacific plates has dominated the Cenozoic tectonic setting of eastern Papua New Guinea (Fig. 1; Benes et al., 1994; Pegler et al., 1995; Tregoning et al., 1998; Wallace et al., 2004). This convergence led to the northward subduction and (U)HP metamorphism of a rifted fragment of the northeast part of the Jurassic–Cretaceous Australian continental margin (including the rocks studied in this paper) beneath an island arc (variously called the Cape Vogel, Dabi or Inner Melanesian arc). The convergence caused southwest emplacement of the arc onto what is now the southeastern peninsula of Papua New Guinea; the exposed substrate of that arc is the Papuan ultramafic belt (PUB; Davies and Smith, 1971; Davies, 1980; Davies and Jacques, 1984; Davies and Warren, 1992; Hill and Baldwin, 1993; Van Ufford and Cloos, 2005). The collision began by 58 Ma (Lus et al., 2004), as dated by $^{40}Ar/^{39}Ar$ of hornblende extracted from the metamorphic sole, and apparently ceased by 35–30 Ma, based on cooling ages of the underlying Owen–Stanley metamorphics and the age of clastic material derived from erosion of the collision belt (Worthing and Crawford, 1996; Smith and Davies, 1976; Rogerson et al., 1987; van Ufford and Cloos, 2005).

Since this collision, the Australian–Pacific plate-boundary zone near Papua New Guinea has fragmented into several microplates (Fig. 1). The tectonic setting is further complicated by the rapid northward subduction of the Solomon Sea plate along the New Britain Trench since at least 6 Ma, which resulted in rifting of the Woodlark Plate from the Australian plate and sea-floor spreading in the Woodlark basin, east of the Papuan Peninsula (Weissel et al., 1982; Fang, 2000; Taylor and Huchon, 2002; Wallace et al., 2004; Westaway, 2007). Spreading is propagating westward, where it transitions into a continental rift ~30–100 km east of the D'Entrecasteaux Islands (Fig. 1; Taylor et al., 1999). The continental crust of southeastern PNG is inferred to have extended ~220 km since ~6 Ma (Taylor et al., 1999); crustal thickness decreases from ~30 to 35 km beneath the southwest and northeast flanks of the rift to ~26–29 km beneath domes (see below) exposed on the D'Entrecasteaux Islands in the central part of the rift (Abers et al., 2002; Ferris et al., 2006). Little et al. (2011) argued that the similarity in crustal thickness across the rift implies that the lower crust is weak and has flowed out from the rift margins on a several million-year timescale (e.g., Bird, 1991). These deformed lower crustal rocks are now exposed on the D'Entrecasteaux Islands.

2.2. D'Entrecasteaux Islands

The D'Entrecasteaux Islands lie in the center of the continental Woodlark rift zone and expose (U)HP eclogite and migmatitic quartzofeldspathic gneisses in the lower plates of several domes (Fig. 2; Davies and Warren, 1988; Hill et al., 1992). The domes are located on Fergusson and Goodenough Islands and are bounded by active normal faults on their northeast flanks. These 30–40° dipping faults cut an older, more gently dipping, regionally extensive fault zone. This fault zone is inferred to have initiated in the Paleogene as the basal thrust of the PUB. Later reactivation of the fault zone in the late Neogene is expressed by a profound metamorphic juxtaposition of UHP rocks beneath upper crustal rocks of the PUB (Little et al., 2011). The hanging wall of this fault zone consists of fault-bounded slivers of ultramafic rock, commonly thought to represent a part of the Papuan Ultramafic Belt. The Belt has resided at shallow crustal levels since at least the early Miocene (Davies and Warren, 1988; Hill, 1994). In contrast, strongly deformed lower-plate gneisses that host mafic blocks were subjected to regional eclogite-facies metamorphism in the late Miocene to Pliocene, followed by widespread amphibolite-facies metamorphism (and partial melting) during exhumation (more detailed summary below).

The lower plates of the domes are composed of migmatitic quartzofeldspathic gneiss that encloses 5–10 vol.% deformed mafic blocks; some of these blocks are—or once were—eclogite, but most are now amphibolite. The structurally higher carapace of the domes' lower plate (< 1 km thick) is strongly foliated and lineated, whereas foliation in the core of the domes is more chaotic. The domes contain leucosomes and dikes that increase in volume structurally downward (~15 vol.% average in the carapace, increasing to ~70 vol.% in the deeply eroded core of Goodenough dome; Table 1). For the samples dated and described herein, "leucosome" refers to quartzofeldspathic layers

Table 1
Proportion of leucosome and dike exposed at sample localities throughout the D'Entrecasteaux domes

Sample	Location	Easting (m)[a]	Northing (m)[a]	Percentage melt[b]	Percentage dike[b]	Percentage dike and melt[b,c]
PNG10024	Goodenough carapace	202,458	8,969,364	2	–	–
PNG06028	Goodenough core	183,898	8,961,495	47	2	49
PNG06034	Goodenough core	199,663	8,967,706	–	69	–
PNG06039	Goodenough core	198,635	8,967,405	–	54	–
PNG10033	Goodenough core	200,982	8,968,532	–	–	38
PNG10034	Goodenough core	200,727	8,968,649	27	2	–
PNG10039-01	Goodenough core	198,221	8,967,202	–	28	–
PNG10039-02	Goodenough core	198,221	8,967,202	–	32	–
PNG09002f	Mailolo carapace	227,854	8,963,870	–	16	–
PNG09020	Mailolo carapace	227,631	8,963,533	–	11	–
PNG09020c	Mailolo carapace	227,631	8,963,533	–	61	–
PNG09005	Mailolo core	227,930	8,960,496	–	–	12
PNG09008	Mailolo core	227,845	8,959,248	–	–	11
PNG09010	Mailolo core	227,888	8,958,859	11	–	–
PNG09014	Mailolo core	227,915	8,960,382	15	–	–
PNG09019	Mailolo core	227,670	8,961,159	–	–	9
PNG09035	Mailolo core	229,698	8,953,526	10	–	–
PNG09037	Mailolo core	229,753	8,953,886	6	18	24
PNG09048	Mailolo core	230,960	8,952,806	9	–	–

[a] GPS measurements using Australia Map Grid 66 (zone 55).
[b] Percentages were measured using a 50 cm^2 quadrat to quantitatively constrain the amount of crystallized melt in leucosome present at an outcrop.
[c] It could not be determined whether the crystallized melt was dike or leucosome; thus, they are listed together.

concordant to the foliation, whereas "dike" implies sharp discordance to the foliation. The leucosomes are interpreted as crystallized melt based on (Little et al., 2011): (1) coarse-grained, euhedral plagioclase (most with fine oscillatory zoning) and/or hornblende that are internally nondeformed; (2) grain long axes rotated towards parallelism with the shear zone boundaries in the middle of the shear zones (tiling of grains); (3) melanocratic borders enriched in coarse-grained hornblende or garnet; and (4) diffuse or nebulitic margins. The deformation in the core of the domes is interpreted to have been coeval with partial melting and with the intrusion of the abundant dm- to m-thick granodioritic to leucogranitic dikes based on a variety of microstructures, including prism-[c] slip lattice-preferred orientations and chessboard-subgrains in quartz, and shape-preferred orientations of euhedral (magmatic) feldspar crystals. All these microstructures suggest high-temperature deformation in the presence of intergranular melt (Fig. 3; Little et al., 2011).

Largely non-deformed granitoid plutons (e.g., the Omara pluton; Baldwin and Ireland, 1995) are the largest bodies of igneous rock and locally cut the D'Entrecasteaux Islands fault zone (Fig. 2). The plutons have granodioritic to leucogranitic compositions similar to the migmatitic gneisses and overlapping initial $^{87}Sr/^{86}Sr$ isotopic ratios of 0.7038–0.7060 (Korchinski, 2012), consistent with the plutons representing local melts of the host gneisses.

The eclogites that are found throughout the lower plates of the domes achieved peak (U)HP conditions of ~700 °C and 27 kbar (Monteleone et al., 2007; Baldwin et al., 2008), although retrogression of the eclogites is extensive, rendering assessment of peak metamorphic conditions difficult. To date, only one coesite-bearing eclogite has been found (Baldwin et al., 2008). Secondary ion mass spectrometry (SIMS) U–Pb in situ dating of zircon in this eclogite indicated (U)HP metamorphism at 7.9 ± 1.9 Ma ($^{238}U/^{206}Pb$–$^{207}Pb/^{206}Pb$ Tera–Wasserburg intercept age; Monteleone et al., 2007), as does a Lu–Hf garnet—whole rock age of 7.1 ± 0.7 Ma (Zirakparvar et al., 2011). Retrogressed eclogites yielded U–Pb zircon SIMS dates that are young from east to west: 4.3 ± 0.4 Ma on Mailolo Dome, Fergusson Island to 2.1 ± 0.5 Ma on Goodenough Dome, Goodenough Island ($^{238}U/^{206}Pb$–$^{207}Pb/^{206}Pb$ Tera–Wasserburg intercept ages; Baldwin et al., 2004; Monteleone et al., 2007). Trace-element analyses of zircons extracted from the HP eclogites revealed no negative Eu anomaly and a flat HREE pattern (Monteleone et al., 2007), indicative of zircon (re)crystallized at high pressure (e.g., Rubatto, 2002).

Subsequent to the UHP metamorphism, the eclogites underwent near-isothermal decompression to 7–14 kbar during rapid exhumation and (ultimately) dome formation (Hill and Baldwin, 1993; Baldwin et al., 2004; Baldwin et al., 2008; Korchinski, 2012). $^{40}Ar/^{39}Ar$ thermochronology on hornblende, white mica and biotite extracted from mainly felsic gneiss and granodiorite throughout the Islands have yielded dates from 3.9 ± 0.3 Ma – 1.5 ± 0.5 Ma, recording the rapid cooling and exhumation of the domes (Baldwin et al., 1993).

In this study, we focus on the Mailolo Dome of northwest Fergusson Island, where the coesite-bearing eclogite was discovered (Fig. 2; Baldwin et al., 2008), to study the role of partial melting in UHP exhumation. We have analyzed leucosomes and granitoid dikes with a variety of textures from different structural levels of the dome, and we report their ages relative to UHP metamorphism and subsequent exhumation.

3. Approach

Samples were collected from two main localities in Mailolo Dome on Fergusson Island. The first, Tumagabuna Island, is on the southwest flank of the dome off the coast (Fig. 2). This islet consists of core-zone rocks: granodioritic orthogneiss, foliation-parallel leucosomes and discordant granite–granodiorite dikes (some of which are pegmatitic), as well as the coesite-bearing eclogite (Baldwin et al., 2008). At the second locality, Mwadeia Gorge, on the northeastern margin of the dome (Fig. 2), samples were collected from the north and south flanks of the dome, including both the carapace and the core of the dome.

The goal of the study is to obtain the most accurate and precise results for the timing of the metamorphism and the melt crystallization. While in situ geochronometric methods (e.g., ion microprobe and ICPMS) can detect gross inheritance patterns within complex zircon crystals, typical spot analyses have two sigma errors on the $^{206}Pb/^{238}U$ dates that are typically more than an order of magnitude less precise than with the TIMS method. There is always a trade-off between precision and spatial resolution;

thus for this study, we have chosen to use both LA-ICPMS for coupled trace-element/U–Pb analyses, but rely on TIMS geochronology for the most reliable geochronological constraints. For all methods, the low abundance of ^{207}Pb in small, relatively low U zircons is an analytical challenge and the uncertainty in the ^{207}Pb/^{235}U date is much larger than the ^{206}Pb/^{238}U date (Fig. 4). We consider the analyses to be at the limits of precision and accuracy.

The Tumagabuna island coesite-bearing eclogite was previously dated in situ by ion microprobe; nine analyses on four zircons yielded a ^{238}U/^{206}Pb–^{207}Pb/^{206}Pb Tera–Wasserburg intercept age of 7.9 ± 1.9 Ma (MSWD=9.2; Monteleone et al., 2007). The high MSWD reflects dispersion of the data beyond that which can be explained by quoted analytical uncertainties; the individual ^{206}Pb/^{238}U dates range from 11.5 ± 1.7 Ma to 5.9 ± 0.8 Ma. Discounting analytical problems, this dispersion suggests real variation in the dates of the zircon spots or the composition of the common Pb used to correct the measured ratios, making the dates difficult to interpret. In either case, the individual common Pb corrected ^{206}Pb/^{238}U dates are the best way to view this data. A Lu–Hf garnet–whole rock date of 7.1 ± 0.7 Ma on the same rock falls in the middle of the SIMS data (Zirakparvar et al., 2011). To understand this important coesite eclogite further, we analyzed zircon from sample PNG08010F, from the same locality using CA-TIMS and LA-ICPMS zircon geochronology (see the supplementary material for detailed instrument methodology). For the CA-TIMS analyses, the low amounts of radiogenic Pb—0.14–0.03 pg for individual zircons—and the need for very low laboratory blanks makes these analyses extremely challenging and led to calculated errors on ^{206}Pb/^{238}U dates of 0.002–1.2 Ma (Fig. 5; Table 2).

The LA-ICPMS analyses were all in situ, one spot per grain, and we examined zircons in a thin section that spans the fresh and retrogressed parts of the eclogite. Retrogression produced partial omphacite and garnet decomposition to amphibole and plagioclase (Fig. 6). Using a FEI Quanta 400f scanning-electron microscope at UCSB, we identified zircons included in fresh omphacite and garnet and in symplectite surrounding partially decomposed omphacite. We then used two ICPMSs (see online supplementary material) for measurement of U–Th–Pb isotopic ratios and REE abundances. Measuring the trace elements from the same compositional domain as U–Th–Pb isotopic ratios allows us to place each date into a petrologic context; e.g., the slope of

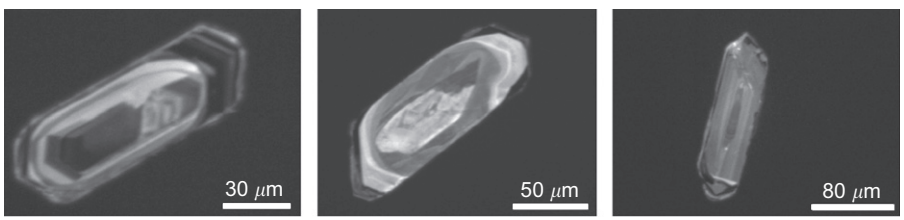

Fig. 4. Cathodoluminescence images of zircons from the PNG leucosomes and dikes. Oscillatory zoning, suggesting magmatic growth, is present in a majority of the grains.

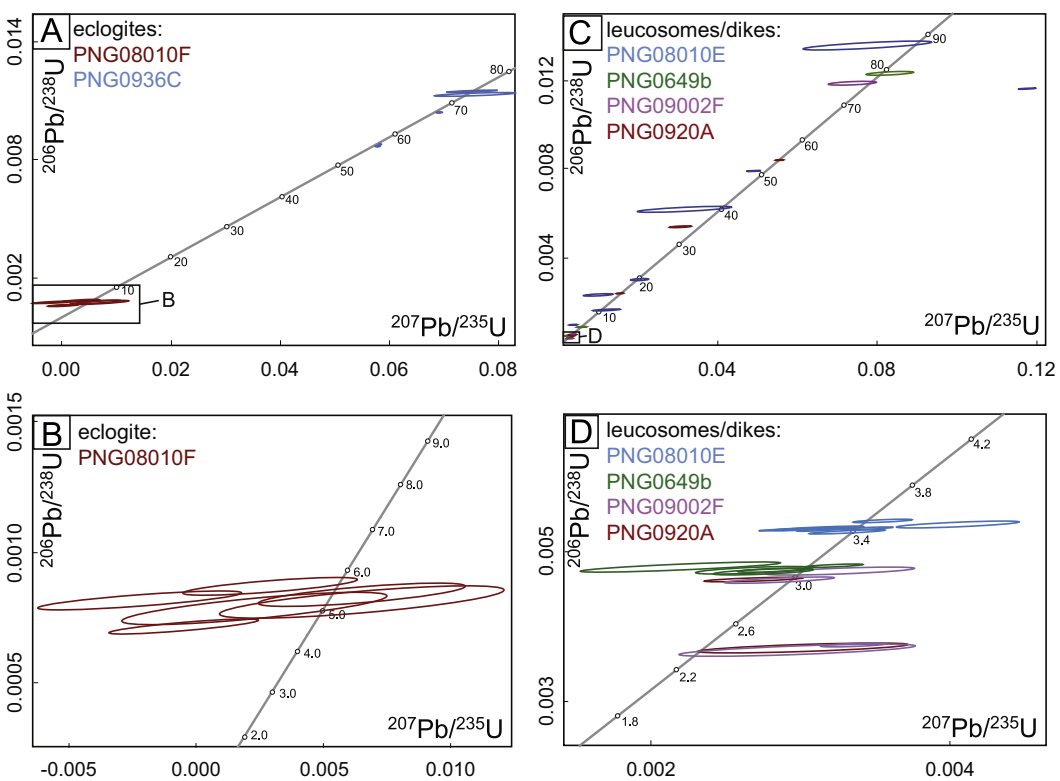

Fig. 5. Concordia diagrams showing U–Pb zircon CA-TIMS analyses for the eclogites, leucosomes, and dikes: (A) all the data for the two eclogite samples, PNG08010F and PNG09036C; (B) inset for Pleistocene–Pliocene eclogite dates; (c) all the data for the leucosome and dike samples, PNG08010E, PNG0649b, PNG0920A and PNG0920C; and (D) inset for Pliocene leucosome and dike dates. Each ellipse represents a single zircon analysis and the 2-sigma confidence for the analytical uncertainties. The dates on concordia are listed in Ma.

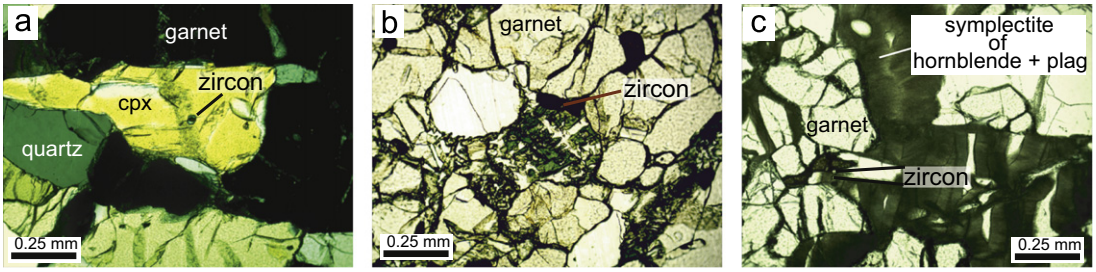

Fig. 6. Photomicrographs showing the textural location of zircon in the coesite-bearing eclogite. (a) Fresh eclogite, where zircon is included in clinopyroxene; (b) a transition region, where clinopyroxene has partly broken down to amphibole and plagioclase; (c) retrogressed rind of the eclogite, where clinopyroxene is nearly completely replaced by a symplectite of amphibole + plagioclase.

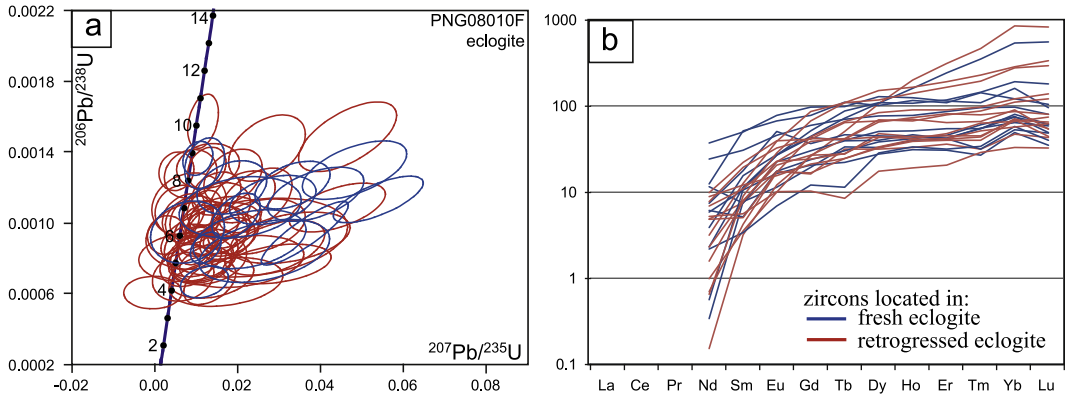

Fig. 7. LA-ICPMS results for the coesite-bearing eclogite (PNG08010F). (a) Concordia diagram showing the U–Pb zircon data with 2-sigma errors collected using a multi-collector ICPMS; (b) REE compositions of the same zircons from (a). Red designates zircons from the retrogressed rim (including the transition area shown in Fig. 6b), and blue represents zircons within fresh clinopyroxene or garnet; both textural zones yield the same dates and REE patterns. (For interpretation of the references to color in this figure caption, the reader is referred to the web version of this article.)

the heavy rare earth element (HREE) pattern reflects whether the zircon crystallized in the presence or absence of garnet, and the strength and sign of a Eu anomaly reflect the presence or absence of plagioclase (e.g., Rubatto and Hermann, 2003). The LA-ICPMS results are presented in a standard concordia diagram in Fig. 7 and Tables 3 and 4, and the zircon CA-TIMS data for the eclogites, leucosomes, and dikes in Fig. 5 and Table 2. The purpose of the LA-ICPMS analyses was to obtain trace-element and U–Pb data from the same volume, not high precision U–Pb geochronology.

4. Results

4.1. Eclogites

Eight zircons extracted from the coesite-bearing eclogite yielded $^{206}Pb/^{238}U$ CA-TIMS dates, corrected for initial Th exclusion, from 5.82 ± 0.20 Ma to 4.78 ± 0.17 Ma (Fig. 5A and B). Twenty-three individual spot in situ LA-ICPMS measurements yielded $^{206}Pb/^{238}U$ dates from 7.4 ± 1.1 Ma to 4.1 ± 1.3 Ma from the fresh portion of the eclogite, and the zircons in the altered parts of the sample reveal $^{206}Pb/^{238}U$ dates of 9.1 ± 0.6 Ma to 3.8 ± 1.0 Ma (Fig. 7a). Most of the zircons do not have a distinct negative Eu anomaly, and most have a flat HREE pattern (Fig. 7b).

Zircons were also extracted for CA-TIMS analysis from an eclogite on the south flank of Mailolo dome, about 15 km east of the UHP locality. The sample, PNG09036C, is retrogressed, with ~10% amphibole and plagioclase. The $^{206}Pb/^{238}U$ dates range from 73.85 ± 0.17 Ma to 55.83 ± 0.05 Ma ($n=6$; Fig. 5A and B) and do not constrain the timing of metamorphism. Some zircons have a relatively complex zoning pattern (Fig. 4), suggesting a complex thermal/growth history.

4.2. Leucosomes and dikes

Variably deformed dikes and leucosomes were also collected from Tumagabuna Island as well as Mwadeia Gorge (Fig. 3). From Tumagabuna Island, a 10 cm-thick foliation-discordant dike (PNG08010E) was sampled from within the granodioritic orthogneiss that hosts the coesite-bearing eclogite. This sample is strongly deformed, with biotite defining an amphibolite-facies fabric. Six zircons analyzed by CA-TIMS yielded a cluster of $^{206}Pb/^{238}U$ dates from 3.49 ± 0.01 Ma to 3.40 ± 0.02 Ma (Fig. 5C and D). A few older zircons have $^{206}Pb/^{238}U$ dates of 86.86 Ma to 6.33 Ma ($n=8$; Fig. 5C).

The remaining migmatitic samples were collected from the north and south flanks of the Mailolo dome and represent a deformation suite, from intensely to weakly deformed leucosomes and dikes. The granodioritic leucosome, PNG0649b, is a strongly deformed, foliation-parallel sheet within the carapace-zone gneisses. Zircons yielded $^{206}Pb/^{238}U$ CA-TIMS dates of 3.10 ± 0.01 Ma to 3.06 ± 0.02 Ma (Fig. 5C and D). Two zircons yielded older $^{206}Pb/^{238}U$ dates of 5.69 ± 0.07 Ma and 78.80 ± 0.45 Ma (Fig. 5c), indicating assimilation of older material; the oldest of which has a minimum age of 78.8 Ma. Nearby, a strongly deformed and boudinaged granodioritic dike (PNG0920A) within the carapace zone gneiss has rare zircons; five were dated. Two grains have $^{206}Pb/^{238}U$ dates of 34.73 ± 0.17 Ma and 15.45 ± 0.06 Ma, and the other three are 2.99 ± 0.02 Ma, 2.98 ± 0.02 Ma, and 2.39 ± 0.05 Ma (Fig. 5C and D). A weakly deformed (tabular, non-boudinaged, nonfolded) granodioritic dike (PNG0920C) from this region reveals fold mullions at the contact between the dike and the quartzofeldspathic host gneiss, indicating minor post-intrusion deformation. Four zircons have $^{206}Pb/^{238}U$ dates ranging from 2.416 ± 0.004 Ma to 2.481 ± 0.007 Ma (Fig. 5C and D), whereas another is 53.94 ± 0.09 Ma. Finally, a discordant, ~30 cm-thick granodioritic dike, PNG09002F, was analyzed. The sample is ~20°

discordant to foliation; flanking fold structures on its margin indicate weak post-intrusion deformation (e.g., Passchier, 2001). Two of the zircons are young (2.37 ± 0.06 Ma and 2.42 ± 0.02 Ma), three are slightly older (2.98 ± 0.03 Ma; 3.06 ± 0.03 Ma; 3.06 ± 0.07 Ma; Fig. 5g), and one gave a $^{206}Pb/^{238}U$ date of 76.03 ± 0.41 Ma (Fig. 5C and D).

5. Discussion

5.1. Time of UHP metamorphism

During the Paleocene, a rifted fragment of Jurassic–Cretaceous Australian-margin sediments was subducted to mantle depths (Davies and Warren, 1992; Hill and Baldwin, 1993), and this material is now exposed as the migmatitic gneisses and eclogite pods in the D'Entrecasteaux Islands. Similar composition, but lower-grade, pumpellyite–actinolite and blueschist-facies accreted rocks of the Owen–Stanley metamorphics occur beneath the PUB on the Papuan Peninsula mainland to the southwest (Fig. 1). These Australian margin-derived protoliths include the Late Cretaceous Gorupu and Emo metabasalt units on the Papuan mainland (e.g., Smith and Davies, 1976; Davies, 1980; Smith, 1982; Davies and Jacques, 1984; Davies and Williamson, 1998; Lus et al., 2004; Daczko et al., 2009). Late Cretaceous inherited and nearly concordant zircons from eclogite PNG09036C (Fig. 5A) are consistent with a similar protolith for a HP eclogite of the D'Entrecasteaux islands.

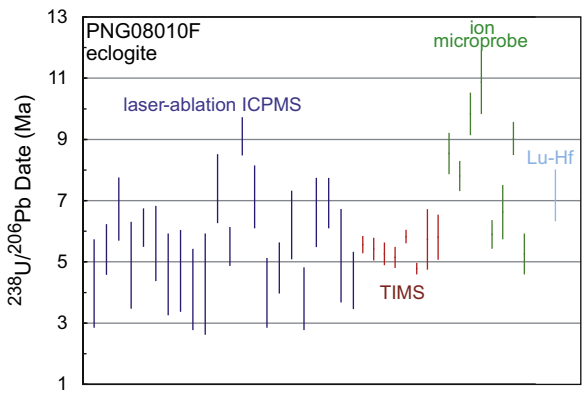

Fig. 8. Individual zircon results from the coesite-bearing eclogite, PNG08010F obtained via four techniques: laser-ablation ICPMS (includes zircons from the fresh and retrogressed part of the rock), CA-TIMS, SIMS (Monteleone et al., 2007), and Lu–Hf (Zirakparvar et al., 2011).

Prior to this study, the PNG coesite-bearing eclogite was interpreted to have recrystallized at UHP at ~7 Ma, based on a Lu–Hf garnet–whole rock date (Zirakparvar et al., 2011) and $^{206}Pb/^{238}U$ SIMS dates from 11.5 ± 1.7 Ma to 5.9 ± 0.8 Ma (Monteleone et al., 2007). The new CA-TIMS $^{206}Pb/^{238}U$ dates from the same rock are younger and define a narrow range: 5.60 ± 0.22 Ma – 4.61 ± 0.18 Ma (Fig. 5B); whether those represent eclogite- or post-eclogite facies recrystallization is unknown. The LA-ICPMS $^{206}Pb/^{238}U$ dates from 9.1 ± 0.6 Ma to 3.8 ± 1.0 Ma are similar to the SIMS data (Fig. 8). However, it is difficult to assess the significance of the wide dispersion in the U–Pb dates by ICPMS, as there is no evidence that altered or unaltered parts of the eclogite yield systematically different dates (Fig. 7a). Most of the zircons analyzed by ICP have REE signatures compatible with (re)crystallization in the presence of garnet and absence of feldspar, but the variations in REE among the zircons indicate disequilibrium between zircon and coexisting phases, inheritance of a REE pattern, or resetting of REE (Fig. 7b). There are no obvious correlations between trace-element concentrations and U–Pb dates.

In summary, the Lu–Hf date is older than the zircon TIMS dates and many of the SIMS and ICPMS dates (Fig. 8). At this time, it is hard to evaluate the greater dispersion seen in the in situ data, and it will require more CA-TIMS geochronology. These data from in situ analysis of eclogitic zircon are permissive of an eclogite-facies event that began by 9.1 ± 0.6 Ma and ended by 3.8 ± 1.0 Ma or that the younger dates reflect post-eclogite facies recrystallization. Overall, Fig. 9 summarizes the geochronology from Fergusson Island and shows the differences between the in situ methods and CA-TIMS. The CA-TIMS data for the three main events, UHP metamorphism, crystallization of strongly deformed leucosomes and dikes, and crystallization of the weakly deformed dikes are consistent with field relationships and thermochronology. In comparison, the ICPMS and SIMS analyses yield a much broader range of dates that overlap with younger events dated by TIMS and Ar–Ar (Fig. 9). In any case, using a white mica Ar–Ar cooling age from Tumabaguna Island (Baldwin et al., 1993), the subducted crustal material was cooled to ~300 °C by 3.5 ± 0.1 Ma at the coesite–eclogite locality.

5.2. UHP–HP metamorphism and exhumation

The UHP–HP eclogites and gneisses in Papua New Guinea crop out within an active rift, which must have had an impact on the

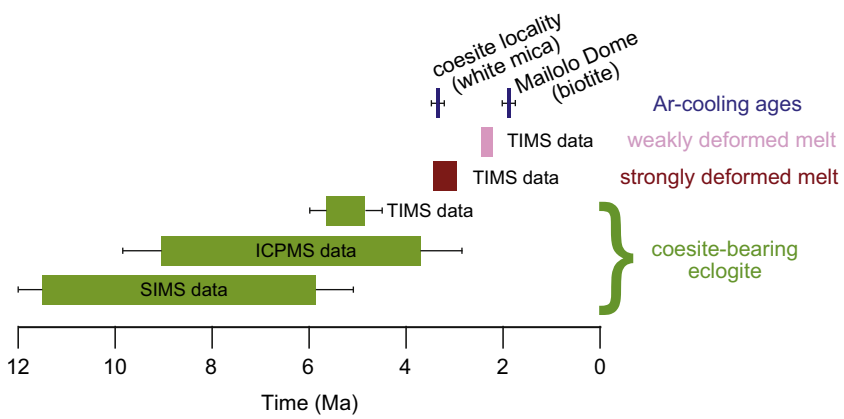

Fig. 9. Timeline of tectonometamorphic events on Fergusson Island, Papua New Guinea, as recorded by U–Pb SIMS, ICPMS, and TIMS data (this study; Monteleone et al., 2007) and $^{40}Ar/^{39}Ar$ data (Baldwin et al., 1993). The timeline is divided into UHP metamorphism, based on the coesite-bearing eclogite (in green), the partial melt crystallization dates from variably deformed leucosomes and dikes (in red and pink), and the Ar-cooling ages (in blue) from two localities: the coesite-bearing eclogite locality and Mailolo Dome. The lines extending from either end of the boxes represent the + and – of the 2-sigma errors for the oldest and youngest dates, respectively; where not shown, the errors are smaller than the symbol. (For interpretation of the references to color in this figure caption, the reader is referred to the web version of this article.)

exhumation of the high-grade rocks. Below, we integrate the tectonic model of Little et al. (2011) with temporal constraints based on the previous SIMS U–Pb dates, the Lu–Hf garnet whole-rock date, and our new U–Pb CA-TIMS and LA-ICPMS results.

The multiple generations of leucosome, dike, and granitoid intrusions throughout the D'Entrecasteaux islands provide a semi-continuous record of the exhumation and dome-formation history. Asthenospheric circulation associated with the westward propagation of the Woodlark spreading ridge probably induced previously subducted nappes of Australian margin material to break away from the paleosubduction channel, where they had been lodged at (U)HP conditions (Little et al., 2011; Ellis et al., 2011). These bodies of Australian margin material then ascended rapidly at >2 cm/yr rates as near vertical diapirs (Little et al., 2011; Ellis et al., 2011) due to their low density relative to the surrounding mantle. Melting associated with the near-isothermal decompression (e.g., Auzanneau et al., 2006) assisted in the buoyant rise. Two- and three-dimensional modeling of UHP diapirs in the Woodlark Rift by Ellis et al. (2010) indicated that partial melting would cause not only a significant reduction in density of the exhuming crustal body (to as low as 2600 kg/m^3), but also a dramatic decrease in viscosity (>4 orders of magnitude less than the mantle). Moreover, the pressure reduction associated with thinning of coevally extending Woodlark Rift above the rising body may have provided another important force aiding exhumation (Ellis et al., 2011).

Subsequent to the buoyancy-driven rise, the former UHP terrane most likely stalled near the base of the crust, as a result of reduced density contrasts (e.g., Walsh and Hacker, 2004). This marks the end of the near-isothermal decompression path and the former UHP terrane most likely began to cool. Stromatic and patch-shaped bodies of leucosome formed subparallel to the foliation, where they later crystallized due to the cooling and were deformed. In addition, abundant granitoid dikes and plutons were emplaced syntectonically and deformed within the main fabric of the gneiss (Fig. 3). The three strongly deformed leucosomes and dikes dated in this study (PNG08010E, PNG06049B and PNG0920A) record the time of crystallization of partial melts, during an early phase of the stalled body of crustal material and lateral extension at the base of the crust, at 3.49 ± 0.01 –3.40 ± 0.02 Ma on Tumagabuna Island and 3.10 ± 0.01 –2.98 ± 0.03 Ma within the Mailolo dome (Fig. 5). All the strongly deformed leucosomes contain plagioclase, suggesting crystallization at crustal levels.

The migmatitic quartzofeldspathic gneisses and the strongly deformed leucosomes and dikes have strong, amphibolite-facies fabrics throughout the domes. Our new geochronological data suggest that the main foliation-forming deformation in the lower crust was younger than (or in part overlapped) the ~3.5–3.0 Ma crystallization of the oldest and strongly deformed leucosomes and dikes. We interpret this as the time of granitoid-dike intrusion that occurred prior to (or during) arrival and stalling of the former-(U)HP body at the base of the crust. This was followed by ductile thinning of the body and its east–west lateral extension parallel to the rift margin, a process modeled by Ellis et al. (2011). This ductile deformation resulted in the formation of the dominant, amphibolite-facies foliation, which was originally subhorizontal (Little et al., 2011).

During the storage of this former-(U)HP material at the base of the crust, at least in the Mailolo dome, there was a second phase of granitoid dike intrusion ~1 my after the initial crystallization of the highly deformed leucosomes and dikes. The weakly deformed dikes record this event. For example, five zircons from dike PNG09002F were dated: three grains are older, 3.06 ± 0.04 Ma, 3.06 ± 0.07 Ma, and 2.98 ± 0.03 Ma, and two grains are younger, 2.42 ± 0.02 Ma and 2.37 ± 0.06 Ma (Fig. 5C and D). We interpret the ca. 3.0 Ma zircons to be inherited and likely reflect that this dike represents a ~3 Ma crystallized leucosome or gneiss that melted. However, the 2.4 Ma dates from PNG0920C and the 2.48–2.37 Ma from the other weakly deformed dike PNG09002F (Fig. 5C and D) record the crystallization during the waning phases of the main amphibolite-facies deformation (Little et al., 2011).

5.3. Papua New Guinea: an unusual UHP terrane?

The (U)HP terrane of Papua New Guinea is unusual in the exposure of Pliocene eclogites, the large amounts of leucosome and dikes, and in its active tectonic setting; however, in other aspects, the PNG eclogites and their history are similar to other UHP terranes. The PNG eclogites, the leucosomes, and the dikes record a multi-phase history that tracks subducted crustal material from mantle depths to the upper crust at cm/yr rates. Melt likely formed during this stage via decompression and may be represented by the early, strongly deformed leucosomes and dikes. Later, perhaps upon reaching the base of the crust, this body stalled, flattened, and was intruded by dikes and pods of partial melt (Little et al., 2011; this study). Subsequently, a combination of buoyancy and upper-crustal extension allowed final emplacement of the former-(U)HP body into the upper crust beneath the PUB. Little et al. (2011) proposed that the Papua New Guinea domes ascended as diapirs. Similar multi-stage exhumation models involving the ascent of crustal diapirs followed by residence in the lower crust have been proposed for some of the other UHP terranes (e.g., Gerya & Stöckhert, 2006), such as northern Tibet (Yin et al., 2007).

There are at least two types of UHP terranes (Kylander-Clark et al., 2012): small terranes subducted and exhumed rapidly (timescales of <10 my) and large terranes subducted and exhumed slowly (timescales of 10–30 my; Rubatto et al., 2003). We now compare the Papua New Guinea UHP terrane to other UHP terranes that achieved similar peak P–T conditions. The Western Gneiss Region (WGR) is a large (~60,000 km^2) UHP–HP body that was exhumed as a coherent slab (e.g., Hacker, 2007; Kylander-Clark et al., 2009). Like PNG, the Western Gneiss Region is thought to have undergone significant coaxial vertical thinning at amphibolite-facies conditions prior to final exhumation mainly driven by upper-crustal extension (e.g., Andersen and Jamtveit, 1990; Andersen et al., 1994; Milnes et al., 1997). The timescales of processes within the Western Gneiss Region, however, are vastly different from PNG, with UHP metamorphism lasting ~25 my (~425–400 Ma; Kylander-Clark et al., 2009; Krogh et al., 2011) and cooling and exhumation another ~20 my (~400–380 Ma; Terry et al., 2000; Krogh et al., 2004; Tucker et al., 2004; Hacker and Gans, 2005; Kylander-Clark et al., 2008), ultimately yielding mean exhumation rates from the mantle to the surface of ~7 mm/y for this very large UHP terrane. In addition, the Western Gneiss Region does not contain plutons associated with the UHP metamorphism, and much of the migmatites formed during earlier tectonic events (e.g., Tucker et al., 1990; Skår & Pedersen, 2003).

Like PNG, the Dora Maira UHP terrane is small and was exhumed at rates of 3.4–1.6 cm/y (e.g., Rubatto and Hermann, 2001). However, unlike PNG, the Dora Maira UHP terrane lacks evidence for significant partial melting associated with either the UHP metamorphism or subsequent decompression; some studies have invoked melting early in the metamorphic history, represented by jadeite–quartzite layers in the massif, but it is not considered to be significant during exhumation (e.g., Schreyer et al., 1987; Sharp et al., 1993; Philippot, 1993). Dora Maira is also different in comparison to PNG in that the exhumation of the UHP rocks is thought to have occurred within a convergent tectonic setting (e.g., Avigad, 1992). Besides PNG, several other UHP

terranes, including Kokchetav and the Bohemian Massif, underwent extensive melting; however, these terranes reached peak temperatures (>1000 °C; Shatsky et al., 1995; Zhang et al., 1997; Massone, 1999) much higher than most UHP terranes (Hacker, 2006), and thus are not directly comparable to a UHP terrane like PNG.

The results from this study of a young UHP terrane that lacks significant tectonic overprinting can be used to understand how a small ($\sim$40–50 km diameter), melt-rich UHP terrane was exhumed: (1) buoyancy-driven exhumation to the base of the crust, accompanied by decompression-driven partial melting; (2) stalling/ponding for $\sim$1 my, accompanied by granodioritic dike emplacement; and (3) final emplacement in the upper crust of an active continental rift within domes caused by plate extension and buoyancy of the ponded partially molten diapir.

6. Conclusions

New U–Pb zircon geochronology from Fergusson Island of Papua New Guinea constrains the timing and duration of (U)HP metamorphism $\sim 5 \pm 2$ Ma for the coesite-bearing eclogite. Following UHP metamorphism, the eclogites rose to the base of the crust, where they stalled, developing a flattening fabric (Little et al., 2011). The strongly deformed, foliation-parallel leucosomes dated in this study reveal that this phase began by $\sim$3.5–3.0 Ma. Weakly deformed, $\sim$2.4 Ma dikes interpreted to have been emplaced during the waning stages of this intermediate (lower-crustal) part of the exhumation indicate that lower crustal storage lasted ca. 1 my. By 1.5 Ma, the domes were exhumed to shallow depths along the D'Entrecasteaux fault, as recorded by apatite (U–Th)/He and fission-track ages (Fitzgerald et al., 2008), revealing exhumation rates of >1 cm/y. Whereas multi-stage exhumation models, including some type of protracted residence at the base of the crust with development of flattening fabrics, have been invoked for many UHP terranes, the D'Entrecasteaux Island leucosomes and dikes preserve a comprehensive record of this exhumation path.

Acknowledgments

We would like to thank Jahan Ramazani, Matt Rioux, and Noah McLean for all their help in the MIT TIMS laboratory and with data handling and reduction. This project was supported by NSF Grants EAR-1019709 (Gordon) and EAR-0607775 (Hacker) and a Marsden Fund Grant 08-VUW-020 (Little). This manuscript greatly benefits from reviews provided by Chris Mattinson and two anonymous reviewers.

Appendix A. Supporting information

Supplementary data associated with this article can be found in the online version at http://dx.doi.org/10.1016/j.epsl.2012.07.014.

References

Abers, G.A., 2001. Evidence for seismogenic normal faults at shallow depths in continental rifts. In: Wilson, R.C.L., et al. (Eds.), Non-volcanic Rifting of Continental Margins. Special Publications of Geological Society, vol. 187; 2001, pp. 305–318.

Abers, G.A., Ferris, A., Craig, M., Davies, H., Lerner-Lam, A.L., Mutter, J.C., Taylor, B., 2002. Mantle compensation of active metamorphic core complexes at Woodlark rift in Papua New Guinea. Nature 418, 862–865.

Andersen, T.B., Jamtveit, B., 1990. Uplift of deep crust during orogenic extensional collapse: a model based on field studies in the Sogn–Sunnfjord region, W Norway. Tectonics 9, 1097–1111.

Andersen, T.B., Osmundsen, P.-T., Jolivet, L., 1994. Deep crustal fabrics and a model for the extensional collapse of the southwest Norwegian Caledonides. J. Struct. Geol. 16, 1191–1203.

Armstrong, R.L., 1991. The persistent myth of crustal growth. Aus. J. Earth Sci. 38, 613–630.

Auzanneau, E., Vielzeuf, D., Schmidt, M.W., 2006. Experimental evidence of decompression melting during exhumation of subducted continental crust. Contrib. Mineral. Petrol. 152, 125–148.

Avigad, D., 1992. Exhumation of coesite-bearing rocks in the Dora Maira massif (Western Alps, Italy). Geology 20, 747–950.

Baldwin, S.L., Ireland, T.R., 1995. A tale of two eras: Pliocene-Pleistocene unroofing of Cenozoic and late Archean zircons from active metamorphic core complexes, Solomon Sea, Papua New Guinea. Geology 23, 1023–1026.

Baldwin, S.L., Lister, G.S., Hill, E.J., Foster, D.A., McDougall, I., 1993. Thermochronologic constraints on the tectonic evolution of active metamorphic core complexes, D'Entrecasteaux Islands, Papua New Guinea. Tectonics 12, 611–628.

Baldwin, S.L., Monteleone, B., Webb, L.E., Fitzgerald, P.G., Grove, M., Hill, E.J., 2004. Pliocene eclogite exhumation at plate tectonic rates in eastern Papua New Guinea. Nature 431, 263–267.

Baldwin, S.L., Webb, L.E., Monteleone, B.D., 2008. Late Miocene coesite–eclogite exhumed in the Woodlark Rift. Geology 36, 735–738.

Benes, V., Scott, S.D., Binns, R.A., 1994. Tectonics of rift propagation into a continental margin: Western Woodlark Basin, Papua New Guinea. J. Geophys. Res. 99, 4439–4455.

Bird, P., 1991. Lateral extension of lower crust from under high topography in the isostatic limit. J. Geophys. Res. 96, 10275–10286.

Chaussidon, M., Albaréde, F., Sheppard, S.M.F., 1987. Sulphur isotope heterogeneity in the mantle from ion microprobe measurements of sulphide inclusions in diamond. Nature 330, 242–244.

Chopin, C., 1984. Coesite and pure pyrope in high-grade blueschists of the Western Alps: a first record and some consequences. Contrib. Mineral. Petrol. 86, 107–118.

Daczko, N., Caffi, P., Halpin, J.L., Mann, P., 2009. Exhumation of the Dayman dome metamorphic core complex, eastern Papua New Guinea. J. Meta. Geol. 27, 405–422.

Davies, H.L., 1980. Folded thrust fault and associated metamorphics in the Suckling–Daymon massif, Papua New Guinea. Am. J. Sci. 280A, 171–191.

Davies, H.L., Smith, I.E., 1971. Geology of eastern Papua. Geol. Soc. Am. Bull. 82, 8299–8312.

Davies, H.L., Jacques, A.L., 1984. Emplacement of ophiolite in Papua New Guinea. Geol. Soc. Lon. Spec. Pub. 13, 341–350.

Davies, H.L., Warren, R.G., 1988. Origin of eclogite-bearing, domed, layered metamorphic complexes (core complexes) in the D'Entrecasteaux Islands, Papua New Guinea. Tectonics 7, 1–21.

Davies, H.L., Warren, R.G., 1992. Eclogites of the D'Entrecasteaux Islands. Contrib. Min. Petrol. 112, 463–474.

Davies, H.L., Williamson, A.N., 1998. Buna, Papua New Guinea, 1:250,000 Geological Series. Geol. Survey Papua New Guinea Explanatory Notes SC/55-3, Port Moresby, Papua New Guinea.

Dobrzhinetskaya, L.F., Eide, E.A., Larsen, R.B., Sturt, B.A., Trønnes, R.G., Smith, D.C., Taylor, W.R., Posukhova, T.V., 1995. Diamond in metamorphic rocks of the Western Gneiss Region in Norway. Geology 23, 597–600.

Eldridge, C.S., Compston, W., Williams, I.S., Harris, J.W., Bristow, J.W., 1991. Isotope evidence for the involvement of recycled sediments in diamond formation. Nature 353, 649–653.

Ellis, S., Little, T.A., Wallace, L., Hacker, B., Buiter, S., 2011. Feedback between rifting and diapirism can exhume ultrahigh-pressure rocks. Earth Planet. Sci. Lett. 311, 427–438.

Ernst, W.G., Liou, J.G., 2000. Overview of UHP metamorphism and tectonics in well-studied collisional orogens. In: Ernst, W.G., Liou, J.G. (Eds.), Ultrahigh-Pressure Metamorphism and Geodynamics in Collision-Type Orogenic Belts. Bellwether Publishing, Columbia, MD, pp. 3–19.

Ernst, W.G., Maruyama, S., Wallis, S., 1997. Buoyancy-driven, rapid exhumation of ultrahigh-pressure metamorphosed continental crust. Proc. Natl. Acad. Sci 94, 9532–9537.

Fang, J., 2000. Styles and Distribution of Continental Extension Derived from the Rift Basins of Eastern Papua New Guinea. Ph.D. Thesis, Columbia University, New York.

Ferris, A., Abers, G.A., Zelt, B., Taylor, B., Roecker, S., 2006. Crustal structure across the transition from rifting to spreading: the Woodlark rift system of Papua New Guinea. Geophys. J. Int. 166, 622–634.

Fitzgerald, P.G., Baldwin, S.L., Miller, S.L., Perry, S.E., Webb, L.E., Little, T.A., 2008. Low-temperature constraints on the evolution of metamorphic core complexes of the Woodlark rift system. AGU, EOS Transact., San Francisco, CA.

Gerya, T.V., Stöckhert, B., 2006. Two-dimensional numerical modeling of tectonic and metamorphic histories at active continental margins. Int. J. Earth Sci. 95, 250–274.

Hacker, B., 2006. Pressures and temperatures of ultrahigh-pressure metamorphism: implications for UHP tectonics and H_2O in subducting slabs. Int. Geol. Rev. 48, 1053–1066.

Hacker, B., 2007. Ascent of the ultrahigh-pressure Western Gneiss Region, Norway. Geol. Soc. Am. Special Paper 419, 171–184.

Hacker, B.R., Gans, P.B., 2005. Continental collisions and the creation of ultrahigh-pressure terranes: petrology and thermochronology of nappes in the central Scandinavian Caledonides. Geol. Soc. Am. Bull. 117, 117–134.
Hill, E.J., 1994. Geometry and kinematics of shear zones formed during continental extension in eastern Papua New Guinea. J. Struct. Geol. 16, 1093–1105.
Hill, E.J., Baldwin, S.L., 1993. Exhumation of high-pressure metamorphic rocks during crustal extension in the D'Entrecasteaux region: Papua New Guinea. J. Metam. Geol. 11, 261–277.
Hill, E.J., Baldwin, S.L., Lister, G.S., 1992. Unroofing of active metamorphic core complexes in the D'Entrecasteaux Islands, Papua New Guinea. Geology 20, 907–910.
Korchinski, M., 2012. Ascent of Ultrahigh-Pressure Rocks in Southeastern Papua New Guinea, as Revealed by Ti-in-Quartz Thermometry and Rb–Sr dating. M.S. Thesis. Victoria University of Wellington.
Krogh, T., Kwok, Y., Robinson, P., Terry, M.P., 2004. U–Pb constraints on the subduction-extension interval in the Averøya–Nordøyane area, Western Gneiss Region, Norway. Goldschmidt Conference Abstract.
Krogh, T.E., Kamo, S.L., Robinson, P., Terry, M.P., Kwok, K., 2011. U–Pb zircon geochronology of eclogites from the Scandian Orogen, northern Western Gneiss Region, Norway: 14–20 million years between eclogite crystallization and return to amphibolite-facies conditions. Can. J. Earth Sci. 48, 441–472.
Kylander-Clark, A.R.C., Hacker, B.R., Mattinson, J.M., 2008. Slow exhumation of UHP terranes: titanite and rutile ages of the Western Gneiss Region, Norway. Earth Planet. Sci. Lett. 272, 531–540.
Kylander-Clark, A.R.C., Hacker, B.R., Johnson, C.M., Beard, B.L., Mahlen, N.J., 2009. Slow subduction of a thick ultrahigh-pressure terrane. Tectonics 28, Article Number: TC2003.
Kylander-Clark, A.R.C., Hacker, B.R., Mattinson, C.G., 2012. Size and exhumation rate of ultrahigh-pressure terranes linked to orogenic stage. Earth Planet. Sci. Lett. 321, 115–120.
Labrousse, L., Prouteau, G., Ganzhorn, A.-C., 2011. Continental exhumation triggered by partial melting at ultrahigh pressure. Geology 39, 1171–1174.
Little, T.A., Baldwin, S.L., Fitzgerald, P.G., Monteleone, B., 2007. Continental rifting and metamorphic core complex formation ahead of the Woodlark spreading ridge, D'Entrecasteaux Islands, Papua New Guinea. Tectonics, 26, , http://dx.doi.org/10.1029/2005TC001911.
Little, T.A., Hacker, B.R., Gordon, S.M., Baldwin, S.L., Fitzgerald, P.G., Ellis, S., Korchinski, M., 2011. Diapiric exhumation of Earth's youngest (UHP) eclogites in the gneiss domes of the D'Entrecasteaux Islands, Papua New Guinea. Tectonophysics 510, 39–68.
Lus, W.Y., McDougall, I., Davies, H.L., 2004. Age of the metamorphic sole of the Papuan Ultramafic Belt ophiolite, Papua New Guinea. Tectonophysics 392, 85–101.
Massone, H.-J., 1999. A new occurrence of microdiamonds in quartzofeldspathic rocks of the Saxonian Erzgebirge, Germany, and their metamorphic evolution. In: Proceedings of the Seventh International Kimberlite Conference, pp. 533–539.
Massone, H.-J., 2003. A comparison of the evolution of diamondiferous quartz-rich rocks from the Saxonian Erzgebirge and the Kokchetav Massif: are so-called diamondiferous gneisses magmatic rocks? Earth Planet. Sci. Lett. 216, 347–364.
Milnes, A.G., Wennberg, O.P., Skar, O., Koestler, A.G., 1997. Contraction, extension, and timing in the South Norwegian Caledonides: the Sognefjord transect. In: Burg, J.-P., Ford, M. (Eds.), Orogeny Through Time. Special Publications of Geological Society, vol. 121; 1997, pp. 123–148.
Monteleone, B.D., Baldwin, S.L., Webb, L.E., Fitzgerald, P.G., Grove, M., Schmitt, A.K., 2007. Late Miocene–Pliocene eclogite facies metamorphism, D'Entrecasteaux Islands, SE Papua New Guinea. J. Metam. Geol. 25, 245–265.
Nasdala, L., Massone, H.-J., 2000. Microdiamonds from the Saxonian Erzgebirge Germany: in situ micro-Raman characterization. Eur. J. Mineral. 12, 495–498.
Passchier, C.W., 2001. Flanking structures. J. Struct. Geol. 23, 951–962.
Philippot, P., 1993. Fluid-melt-rock interaction in mafic eclogites and coesite-bearing metasediments: constraints on volatile recycling during subduction. Chem. Geol. 103, 93–112.
Pegler, G., Das, S., Woodhouse, J.H., 1995. A seismological study of the eastern New Guinea and the western Solomon Sea regions and its tectonic implications. Geophys. J. Int. 122, 961–981.
Rogerson, R., Hilyard, D., Finalyson, E.J., Holland, D.S., Nion, S.T.S., Sumaiang, R.S., Duguman, J., Loxton, C.D.C., 1987. The geology and mineral resources of the Sepik headwaters region, Papua New Guinea. Geol. Surv. Papua New Guinea Mem. 12, 1–130.
Rubatto, D., 2002. Zircon trace element geochemistry: partitioning with garnet and the link between U–Pb ages and metamorphism. Chem. Geol. 184, 123–138.
Rubatto, D., Hermann, J., 2001. Exhumation as fast as subduction? Geology 29, 3–6.
Rubatto, D., Hermann, J., 2003. Zircon formation during fluid circulation in eclogites (Monviso, Western Alps): implications for Zr and Hf budget in subduction zones. Geochim. Cosmochim. Acta 67, 2173–2187.
Rubatto, D., Liati, A., Gebauer, D., 2003. Dating UHP metamorphism. In: Compagnoni, R., Carswell, D.A. (Eds.), Ultrahigh-Pressure Metamorphism. European Mineralogical Union, Budapest, pp. 341–363.
Ruppel, C., 1995. Extensional processes in continental lithosphere. J. Geophys. Res. 100, 24187–24215.
Schreyer, W., 1995. Ultradeep metamorphic rocks: the retrospective viewpoint. J. Geophys. Res. 100, 8353–8366.
Schreyer, W., Massone, H.J., Chopin, C., 1987. Continental crust subducted to depths near 100 km: implications for magma and fluid genesis in collision zones. In: Mysen, B.O. (Ed.), Magmatic Processes: Physiochemical Principles. Geochemical Society, University Park, PA, pp. 155–163.
Sharp, Z.D., Essene, E.J., Hunziker, J.C., 1993. Stable isotope geochemistry and phase equilibria of coesite-bearing whiteschists, Dora Maira Massif, Western Alps. Contrib. Min. Petrol. 114, 1–12.
Shatsky, V.S., Sobolev, N.V., Vavilow, M.A., 1995. Diamond-bearing metamorphic rocks of the Kokchetav Massif (Northern Kazakhstan). In: Coleman, R., Wang, X. (Eds.), Ultrahigh-Pressure Metamorphism. Cambridge University Press, Cambridge, MA, pp. 427–455.
Skår, Ø., Pedersen, R.B., 2003. Relations between granitoid magmatism and migmatization: U–Pb geochronological evidence from the Western Gneiss Complex. Norway J. Geol. Soc. Lon. 160, 935–946.
Smith, I.E.M., 1982. Volcanic evolution in eastern Papua. Tectonophysics 87, 315–333.
Smith, D.C., 1984. Coesite in clinopyroxene in the Caledonides and its implications for geodynamics. Nature 310, 641–644.
Smith, I.E., Davies, H.L., 1976. Geology of the southeast Papuan Mainland. Aust. BMR Geol. Geophys. Bull 165, 32.
Sobolev, N.V., 1984. Crystalline inclusions in diamonds from New South Wales, Australia. In: Glover, J.E., Harris, P.G. (Eds.), Kimberlite Occurrence and Origin, vol. 8. Geology Department and University Extension, University of Western Australia, Nedlands, pp. 213–226.
Sobolev, V.S., Sobolev, N.V., 1980. New evidence on subduction to great depths of the eclogitized crustal rocks (in Russian). Dokl. Akad. Sci. USSR 250, 683–685.
Sobolev, N.V., Shatsky, V.S., 1990. Diamond inclusions in garnets from metamorphic rocks: a new environment for diamond formation. Nature 343, 742–746.
Syracuse, E.M., van Keken, P.E., Abers, G.A., 2010. The global range of subduction zone thermal models. Phys. Earth Planet. Interiors 183, 73–90.
Taylor, B., Huchon, P., 2002. Active continental extension in the western Woodlark basin: a synthesis of Leg 180 results. In: Proc. Ocean Drilling Program. Science Results (CD-ROM) 18, 36.
Taylor, B., Goodliffe, A.M., Martinez, F., 1999. How continents break-up: insights from Papua New Guinea. J. Geophys. Res. 104, 7497–7512.
Terry, M.P., Robinson, P., Hamilton, M.A., Jercinovic, M.J., 2000. Monazite geochronology of UHP and HP metamorphism, deformation, and exhumation, Nordøyane, Western Gneiss Region, Norway. Am. Min. 85, 1651–1664.
Tregoning, P., et al., 1998. Estimation of current plate motions in Papua New Guinea from global positioning system observations. J. Geophys. Res. 103, 12181–12203.
Tucker, R.D., Boyd, R., Barnes, S.-J., 1990. A U–Pb zircon age for the Rana intrusion, N. Norway: new evidence of basic magmatism in the Scandinavian Caledonides in Early Silurian time. Norsk Geologisk Tidsskrift 70, 229–239.
Tucker, R.D., Robinson, P., Solli, A., Gee, D.G., Thorsnes, T., Krogh, T.E., Nordgulen, O., Bickford, M.E., 2004. Thrusting and extension in the Scandian hinterland, Norway: new U–Pb ages and tectonostratigraphic evidence 304, 477–532Am. J. Sci. 304, 477–532.
Van Ufford, Q.A., Cloos, M., 2005. Cenozoic tectonics of New Guinea. Am. Association Petrol. Geol. Bull 89, 119–140.
Wallace, L.M., Stevens, C., Silver, E., McCaffrey, R., Loratung, W., Hasiata, S., Stanaway, R., Curley, R., Rosa, R., Taugaloidi, J., 2004. GPS and seismological constraints on active tectonics and arc-continent collision in Papua New Guinea: implications for mechanics of microplate rotations in a plate boundary zone. J. Geophys. Res. 109, B05405, , http://dx.doi.org/10.1029/2003JB002481.
Walsh, E.O., Hacker, B.R., 2004. The fate of subducted continental margins: two-stage exhumation of the high-pressure to ultrahigh-pressure Western Gneiss Region. Norway J. Metam. Geol. 22, 671–687.
Warren, C.J., Beaumont, C., Jamieson, R.A., 2008. Deep subduction and rapid exhumation: role of crustal strength and strain weakening in continental subduction and ultrahigh-pressure rock exhumation. Tectonics 27, TC6002.
Weissel, J.K., Taylor, B., Karner, G.D., 1982. The opening of the Woodlark Basin, subduction of the Woodlark spreading system, and the evolution of northern Melanesia since mid-Pliocene time. Tectonophysics 87, 253–277.
Westaway, R., 2007. Correction to "Active low-angle normal faulting in the Woodlark extensional province, Papua New Guinea: a physical model. Tectonics 26, TC1003.
Worthing, M.A., Crawford, A.J., 1996. The igneous geochemistry and tectonic setting of metabasites from the Emo metamorphics, Papua New Guinea: the record of the evolution and destruction of a back-arc basin. Min. Petrol. 58, 79–100.
Yin, A., Manning, C.E., Lovera, O., Menold, C.A., Xuanhua, C., Gehrels, G.E., 2007. Early Paleozoic tectonic and thermomechanical evolution of ultrahigh-pressure (UHP) metamorphic rocks in the northern Tibetan Plateau, Northwest China. Int. Geol. Rev. 49, 681–716.
Zhang, R.Y., Liou, J.G., Ernst, W.G., Coleman, R.G., Sobolev, N.V., Shatsky, V.S., 1997. Metamorphic evolution of diamond-bearing and associated rocks from the Kokchetav Massif, northern Kazakhstan. J. Metam. Geol. 15, 479–496.
Zirakparvar, N.A., Baldwin, S.L., Vervoort, J.D., 2011. Lu–Hf garnet geochronology applied to plate boundary zones: insights from the (U)HP terrane exhumed within the Woodlark Rift. Earth Planet. Sci. Lett. 309, 56–66.